

Supplementary information

Oxygenation state of the cores during the subsampling

Core RHS-KS-33 was characterized by the presence of black organic matter spots (Fig. 3). An oxidation of these organic matter spots, indicated by a change in color (black spots turned yellow), was observed to occur during the following 24 hours after core splitting. These organic matter spots were also noticed on the twin core MD99-2348, recovered several years before. The difference between the two cores is that core MD99-2348 was split in half onboard, immediately upon arrival on the core deck, and that core RHS-KS-33, was split in half in the laboratory, after 3 days of transport. These observations strongly indicate that the oxic state of both cores (RHS-KS-33 and twin core MD99-2348) was similar, and that the transport at 4°C did not affect the main physical characteristics of the cores. As core KESC9-30 was stored, transported and subsampled under exactly the same conditions and within the same time period, this core should not have been affected nor oxidized during the transport or subsequent subsampling.

Supplementary Tables

Table S1: Location, bathymetry, length and age of studied and reference cores.

Core	Cruise	Latitude	Longitude	Water Depth (m)	Length (cm)	AMS ^{14}C date (cal ka)
<i>Studied cores*</i>						
KESC9-30	ESSCAR9	43°23'.016N	07°44'.187E	2160	828	*calc. age model
RHS-KS-33	RHOSOS	42°41'.596N	03°50'.493E	291	709	*calc. age model
<i>Reference cores*</i>						
KNI-23	NICASAR	43°23'.02N	07°44'.19E	2130	1052	(Jorry et al., 2011)
MD99-2348	IMAGES V	42°69'.300N	03.84'.167E	300	2400	(Sierro et al., 2009)

*Cores were recovered using a Küllenberg piston corer

Table S2: Chemical composition of sediments from Western Mediterranean Sea, at two sites: Gulf of Lions and Ligurian Sea.

	Depth int. (cmbsf)	Na ₂ O (%)	MgO (%)	Al ₂ O ₃ (%)	SiO ₂ (%)	P ₂ O ₅ (%)	SO ₄ ²⁻ (%)	K ₂ O (%)	CaO (%)	TiO ₂ (%)	MnO (%)	Fe ₂ O ₃ (%)	Co (PPM)	Ni (PPM)	Cu (PPM)	Zn (PPM)	As (PPM)	Rb (PPM)	Sr (PPM)	Zr (PPM)	Ba (PPM)	Pb (PPM)	LOI (%)	
Ligurian Sea, KESC9-30																								
3-9	1,03	1,98	9,33	37,29	0,12	0,12	1,25	21,91	0,44	0,05	3,45	10	33	20	65	15	91	513	99	319	53	22,34		
45-52	1,04	1,98	9,04	39,34	0,12	0,14	1,35	21,60	0,44	0,04	3,24	8	26	14	55	10	87	453	105	305	18	21,54		
86-89	0,98	1,96	9,40	38,14	0,13	0,16	1,42	21,65	0,45	0,05	3,52	9	35	18	62	13	89	505	97	330	26	21,68		
101-105	0,96	1,90	9,28	37,34	0,12	0,24	1,43	22,53	0,44	0,04	3,28	10	32	18	59	10	87	514	98	338	19	22,08		
120-125	1,01	1,92	9,38	38,32	0,13	0,18	1,36	21,99	0,45	0,04	3,52	9	38	21	60	11	88	526	105	299	29	21,78		
151-155	0,96	1,87	8,69	37,67	0,12	0,22	1,24	23,00	0,42	0,04	3,16	9	31	18	54	10	83	518	100	300	38	22,58		
182-186	1,01	1,82	8,88	38,99	0,12	0,25	1,30	21,82	0,42	0,05	3,19	9	29	15	53	12	84	494	102	311	34	21,75		
201-205	1,08	2,10	9,82	37,63	0,12	0,23	1,35	21,46	0,47	0,05	3,52	9	37	21	64	12	95	500	97	316	40	22,08		
223-227	1,03	2,05	9,09	36,41	0,12	0,25	1,13	22,99	0,42	0,04	3,25	8	37	18	59	8	86	569	95	313	35	22,88		
251-256	1,03	1,90	9,01	39,69	0,11	0,19	1,30	21,43	0,43	0,05	3,20	8	34	17	56	7	85	506	104	315	30	21,62		
281-286	1,02	2,12	9,50	38,13	0,12	0,15	1,21	21,51	0,45	0,05	3,43	9	41	20	60	6	88	517	106	334	70	22,13		
300-305	1,28	2,50	10,38	40,17	0,12	0,22	1,48	19,10	0,46	0,06	3,86	12	56	21	66	7	98	490	89	344	71	20,11		
321-326	1,01	2,25	9,51	35,82	0,12	0,22	1,15	22,70	0,45	0,06	3,48	10	45	22	62	6	88	521	108	346	68	22,99		
351-356	1,21	2,13	9,31	38,00	0,12	0,23	1,16	21,57	0,40	0,05	3,29	11	44	20	59	6	96	512	87	316	73	22,16		
382-385	1,24	2,05	9,82	38,75	0,12	0,16	1,49	20,50	0,43	0,05	3,49	9	40	20	64	7	109	504	88	345	36	20,97		
402-406	1,20	1,86	9,25	38,69	0,12	0,33	1,45	22,04	0,39	0,05	3,05	8	33	15	56	5	105	511	84	319	35	21,42		
422-427	1,10	2,03	9,31	37,06	0,12	0,33	1,33	22,52	0,41	0,05	3,25	9	37	17	58	8	100	537	82	340	67	22,38		
452-457	1,03	1,80	7,99	36,35	0,12	0,26	1,31	24,83	0,33	0,04	2,66	7	27	13	47	5	83	549	74	312	72	23,14		
483-487	0,88	2,01	8,66	34,61	0,12	0,28	1,24	24,70	0,40	0,04	2,98	8	31	18	57	7	81	554	85	349	48	23,73		
503-507	0,99	2,05	8,93	35,78	0,12	0,25	1,25	23,65	0,42	0,05	3,31	9	35	18	58	8	82	538	88	380	38	23,05		
532-538	1,28	1,45	7,28	40,88	0,11	0,20	1,47	23,76	0,25	0,02	2,23	8	20	9	39	6	75	500	61	373	42	21,26		
563-567	0,85	2,11	8,72	34,16	0,12	0,27	1,16	24,68	0,41	0,05	3,02	9	36	17	58	9	83	575	86	349	53	23,95		
583-587	0,93	1,99	8,27	35,15	0,12	0,39	1,21	24,69	0,37	0,04	3,01	9	34	15	54	17	79	562	87	350	42	23,50		
603-607	1,17	2,40	10,03	38,89	0,13	0,20	1,60	20,56	0,48	0,05	3,71	10	37	20	68	14	97	465	102	462	55	20,68		
633-638	1,31	1,90	9,05	43,46	0,12	0,20	1,66	19,52	0,37	0,04	2,98	9	26	14	54	8	91	435	91	424	64	18,82		
663-667	1,25	2,15	9,90	41,68	0,13	0,23	1,70	19,18	0,45	0,05	3,58	10	35	17	64	11	99	441	120	436	38	19,10		
683-688	1,50	1,85	9,41	48,18	0,14	0,18	1,79	16,98	0,38	0,04	3,11	8	26	13	52	8	94	390	113	426	48	16,50		

703-707	1,73	1,30	8,87	54,38	0,13	0,21	1,89	14,46	0,28	0,03	2,42	8	13	6	35	7	96	336	120	456	55	13,60
723-728	1,29	2,28	10,49	43,10	0,14	0,08	1,77	17,70	0,49	0,05	3,73	11	34	19	70	7	109	415	161	419	84	18,46
752-757	1,26	2,16	10,10	42,30	0,13	0,14	1,80	19,03	0,47	0,05	3,55	9	29	18	66	9	104	433	114	433	40	18,80
782-786	1,36	1,90	9,55	44,90	0,13	0,16	1,80	18,53	0,41	0,04	3,19	8	24	15	56	8	101	424	124	442	53	17,91
808-813	1,28	2,13	9,71	43,97	0,14	0,14	1,85	18,51	0,46	0,05	3,44	9	26	16	62	9	101	422	131	445	58	18,30
Gulf of Lions, RHS-KS-33																						
12-17	1,06	1,95	7,82	35,75	0,12	0,24	1,06	24,60	0,37	0,05	3,09	9	32	10	57	7	76	612	93	291	63	23,95
43-47	1,04	2,59	9,71	39,12	0,13	1,20	1,44	19,94	0,46	0,06	3,66	9	35	14	65	34	93	420	104	441	50	20,14
84-88	1,04	2,93	10,30	38,50	0,14	0,42	1,52	19,76	0,48	0,07	3,60	10	38	18	67	15	99	403	98	396	50	20,99
109-114	1,09	2,83	10,14	38,75	0,14	0,46	1,48	19,60	0,48	0,06	3,61	10	35	16	65	17	97	398	97	410	67	20,76
140-145	1,08	2,68	10,27	37,78	0,14	0,39	1,30	19,50	0,48	0,06	3,66	9	34	17	67	13	99	400	95	424	129	21,99
178-183	1,12	2,53	10,45	38,71	0,13	0,28	1,49	20,00	0,49	0,06	3,71	10	34	16	66	12	100	402	100	411	89	21,22
198-203	1,16	2,51	10,64	39,04	0,13	0,30	1,53	19,27	0,50	0,06	3,77	10	35	16	67	9	103	406	100	425	65	20,84
238-242	1,09	2,37	10,26	38,90	0,13	0,24	1,39	19,76	0,49	0,06	3,63	10	33	16	64	9	98	407	103	399	99	21,07
267-271	1,06	2,42	10,49	40,00	0,14	0,28	1,58	19,30	0,50	0,07	3,84	9	33	15	66	11	98	387	105	396	54	20,11
307-312	1,29	2,47	10,50	40,11	0,14	0,24	1,35	18,64	0,50	0,07	3,81	10	32	16	64	12	98	373	111	392	40	20,36
337-341	1,10	2,48	10,63	41,43	0,14	0,23	1,56	18,27	0,51	0,07	3,79	10	33	15	66	12	100	378	118	396	58	19,43
378-382	1,24	2,36	10,65	41,20	0,13	0,21	1,52	18,11	0,51	0,06	3,82	10	33	16	66	14	101	345	117	386	48	19,73
408-411	1,10	2,37	10,47	39,29	0,14	0,24	1,48	19,45	0,50	0,07	3,76	9	36	16	66	14	100	377	104	375	41	20,54
438-442	1,09	2,52	10,37	38,12	0,13	0,13	1,49	20,26	0,48	0,07	3,76	10	40	16	64	13	97	378	92	353	73	21,27
478-481	1,00	2,46	9,62	35,99	0,13	0,16	1,22	22,04	0,45	0,07	3,44	10	38	14	61	13	89	376	84	335	63	22,79
508-512	0,88	2,36	8,78	33,63	0,13	0,22	1,07	24,47	0,42	0,07	3,23	8	31	12	56	11	81	385	80	329	38	24,37
538-542	1,07	2,41	10,46	37,85	0,13	0,13	1,52	20,74	0,49	0,07	3,66	10	34	13	63	14	95	384	97	363	38	21,24
578-582	1,10	2,40	11,07	38,82	0,14	0,14	1,72	19,70	0,50	0,07	3,88	10	35	15	66	14	103	402	99	400	42	20,40
599-602	1,13	2,42	11,20	37,72	0,13	0,09	1,71	19,94	0,50	0,07	3,79	9	35	16	66	15	105	396	90	392	56	21,02
637-641	1,14	2,41	10,90	38,13	0,13	0,13	1,61	20,09	0,49	0,07	3,90	10	34	15	65	16	99	389	95	385	40	20,88
658-663	1,11	2,48	11,16	38,41	0,14	0,18	1,64	19,80	0,51	0,07	3,97	10	35	15	66	15	101	397	95	392	52	20,07
698-703	1,10	2,49	11,03	37,47	0,13	0,22	1,65	19,76	0,50	0,07	4,10	11	36	14	67	16	104	403	93	407	34	20,76

Supplementary References

- Beaudouin, C., Suc, J. P., Acherki, N., Courtois, L., Rabineau, M., Aliosi, J. C., Sierro, F. J., and Oberlin, C.: Palynology of the northwestern Mediterranean shelf (Gulf of Lions): First vegetational record for the last climatic cycle, *Marine and Petroleum Geology*, 22, 845-863, 10.1016/j.marpetgeo.2005.03.005, 2005.
- Jégou, I.: Comment l'activité turbiditique est-elle enregistrée dans les dépôts de débordement de la ride sédimentaire du Var ?, Université de Bretagne Occidentale, Rapport de DEA, 2004.
- Migeon, S., Savoye, B., and Faugeres, J. C.: Quaternary development of migrating sediment waves in the Var deep-sea fan: distribution, growth pattern, and implication for levee evolution, *Sedimentary Geology*, 133, 265-293, 10.1016/s0037-0738(00)00043-9, 2000.

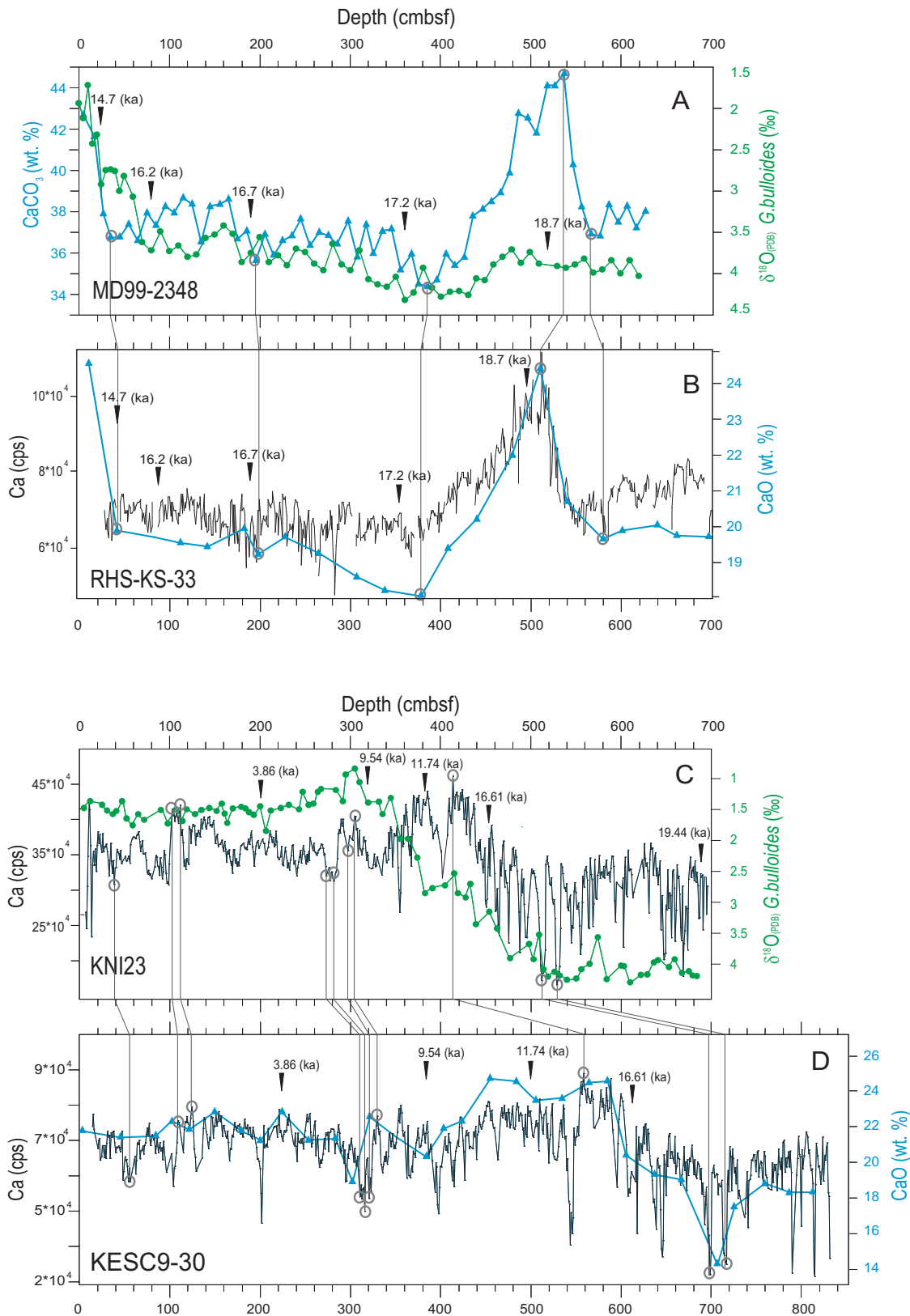


Fig. S1 Age model based on planktonic oxygen isotopes and AMS ^{14}C dates calibrated on the calcium records of twin cores: MD99-2348 and KNI23 (Sierra et al., 2009; Jorry et al., 2011). The green plain circles represent $\delta^{18}\text{O}_{\text{PDB}} \text{G. bulloides}$ record in MD99-2348 (A) and KNI23 (C) cores. The black arrows show the AMS ^{14}C dates (ka cal BP) in twin cores and transposed AMS ^{14}C dates in studied cores. The grey circles point up the calibration peaks of core correlations. Abbreviations: cmbsf, centimeters below the seafloor; cps, counts

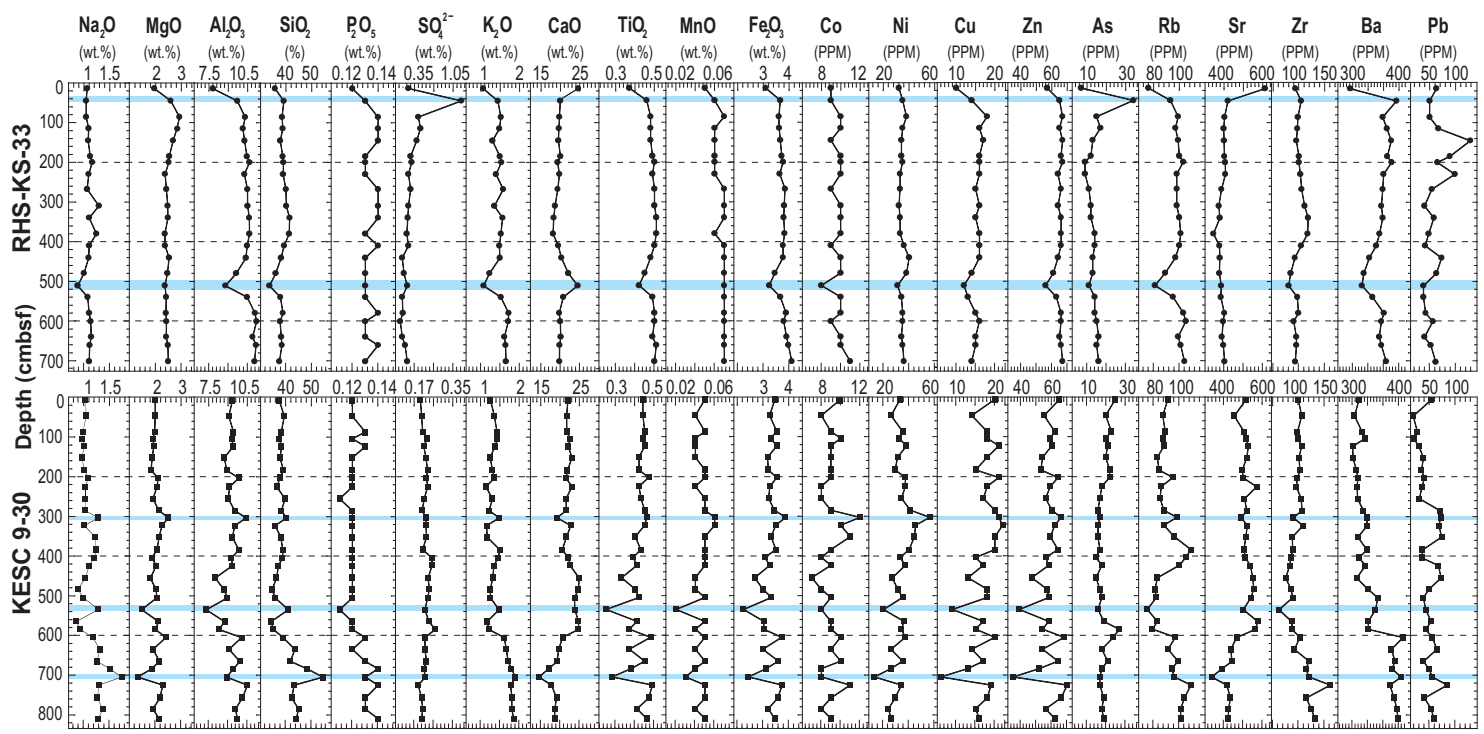


Fig. S2 Elemental composition of the sediment in cores RHS-KS-33 and KESC9-30. The black dots and the black squares represent contiguous samples of ~ 3 cm thick analyzed using WD-XRF. The blue blocks represent important changes in elemental composition profiles.

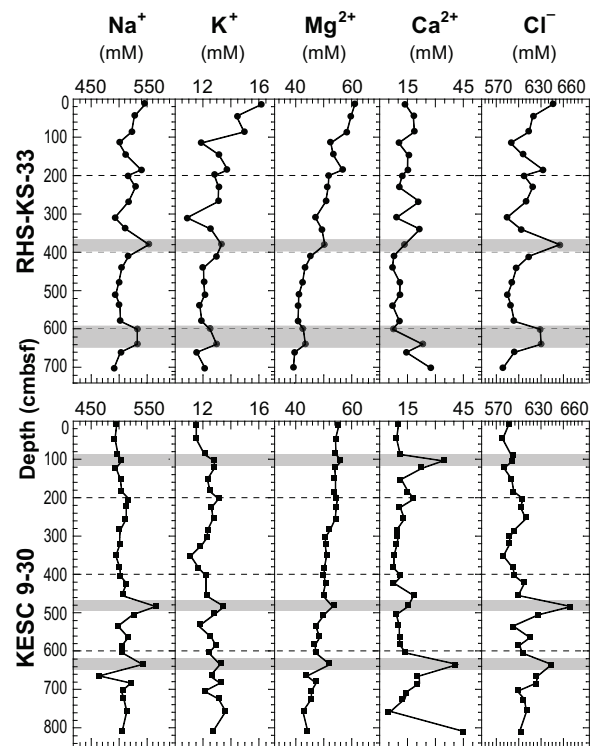
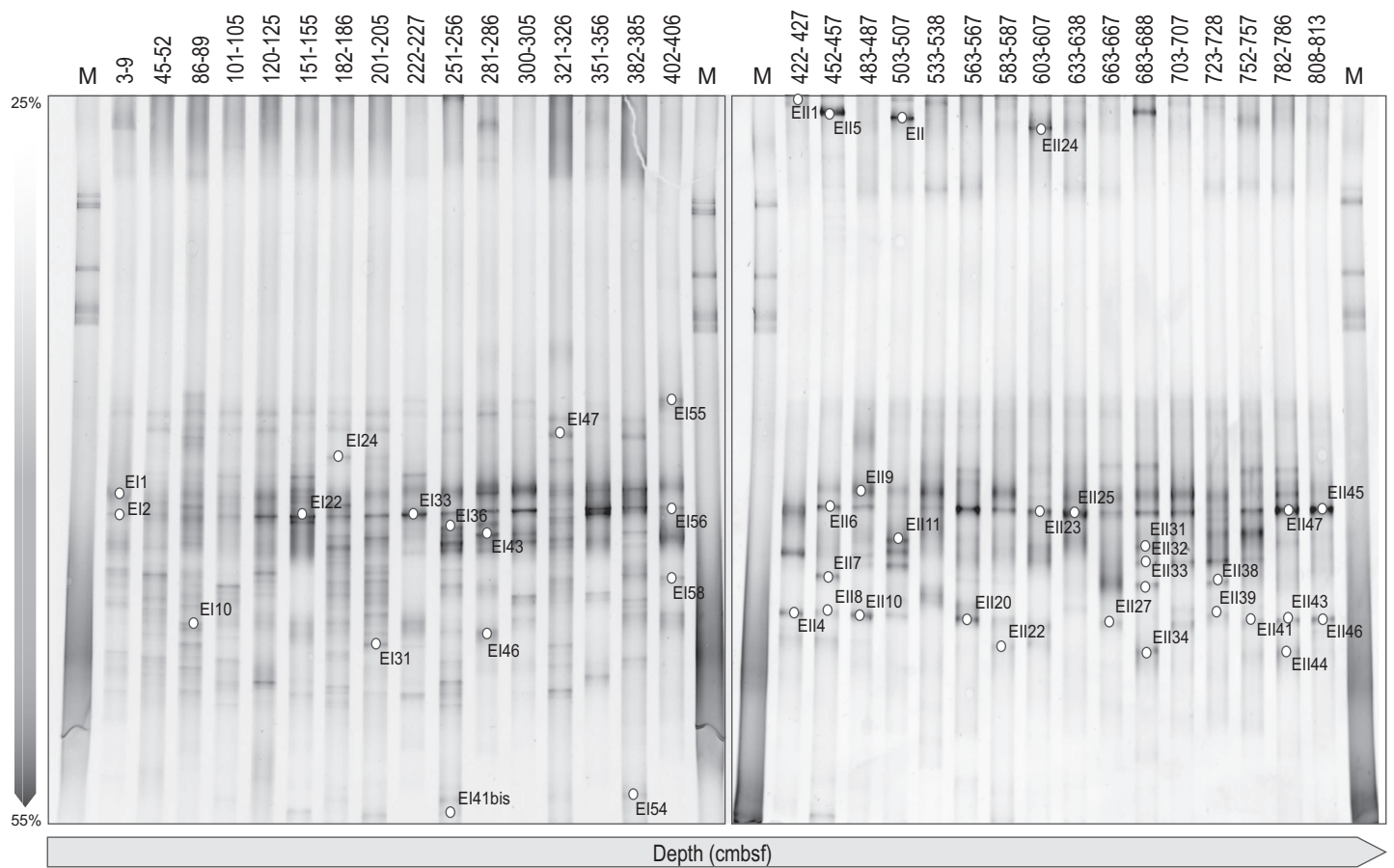


Fig. S3 Depth profiles of geochemical pore water measurements of studied cores. The grey blocks represent important changes of measured ions. Abbreviations: cmbsf, centimeters below the seafloor.

BACTERIA

A KESC9-30



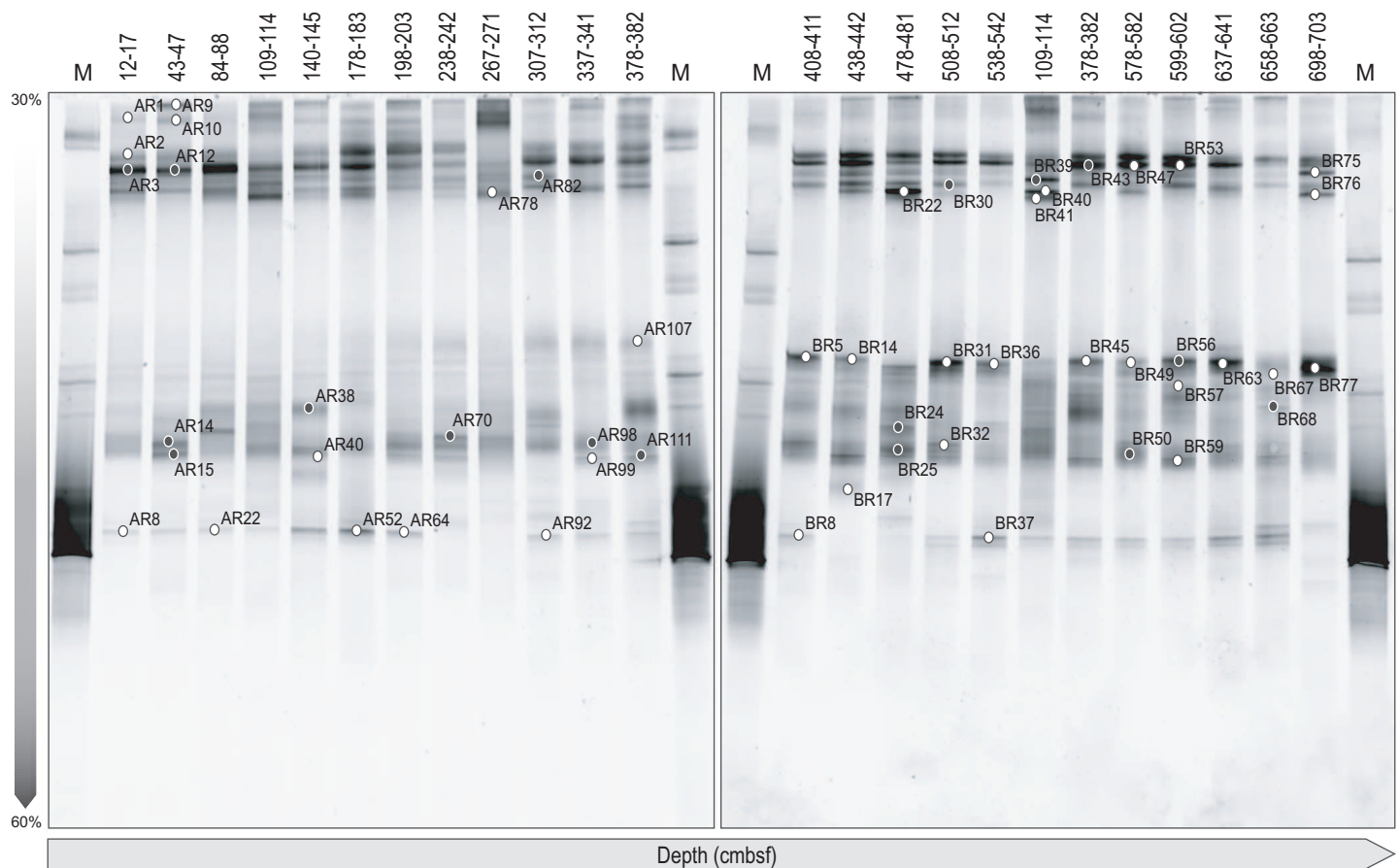
B Sequence similarity of excised DGGE bands

- EI1 *Acinetobacter* sp. (EU275352) 99%, *Moraxellaceae*, *Gammaproteobacteria*
 EI10 Uncultured bacterium clone ODP1251B11.22 (AB177311) 98%, *Dehalococcoidetes*, *Chloroflexi*
 EI22, 56 *Ralstonia* sp. (HQ267096) 98%, 99%, *Ralstoniaceae*, *Betaproteobacteria*
 EI24 Uncultured bacterium clone CK_2C5_23 (EU488454) 96%, *Dehalococcoidetes*, *Chloroflexi*
 EI31 Uncultured bacterium clone EPR3967-orBc49 (EU491796) 90%, *Burkholderiaceae*, *Betaproteobacteria*
 EI33 *Ralstonia* sp. (JF772078) 98%, *Ralstoniaceae*, *Betaproteobacteria*
 EI36 Uncultured bacterium clone ORI-860-18-P_S281-283_185B08 (GU553684) 90%, OP8 candidate division
 EI41bis, 54 Uncultured bacterium clone AMSMV-S1-B5 (FJ649500) 93%, *Chloroflexi*
 EI43 *Acinetobacter* sp. (EU919204) 98%, *Moraxellaceae*, *Gammaproteobacteria*
 EI46, EI8, 27, 41 Uncultured beta proteobacterium clone Kir51gm dB7.2 (HM480181) 99%, 98% *Comamonadaceae*, *Betaproteobacteria*
 EI47 Uncultured bacterium *Mesorhizobium* sp. (EF219052) 99%, *Phyllobacteriaceae*, *Alphaproteobacteria*
 EI55 *Pedobacter* sp. (EF660750) 98%, *Sphingobacteriaceae*, *Bacteroidetes*
 EI58 Uncultured bacterium clone HH1541 (FJ502260) 97%, *Flavobacteriaceae*, *Bacteroidetes*
 EI11 Uncultured bacterium clone ZSB-A2-7 (GU205510) 95%, *Comamonadaceae*, *Betaproteobacteria*
 EI14 *Comamonas* sp. (GU296675) 98%, *Comamonadaceae*, *Betaproteobacteria*
 EI15 *Flavobacterium* sp. (GU138375) 98%, *Flavobacteriaceae*, *Bacteroidetes*
 EI16 Uncultured bacterium clone BIGO950 (HM558883) 99%, *Ralstoniaceae*, *Betaproteobacteria*
 EI17 Uncultured *Burkholderia* sp. clone burk842 (GU123681) 97%, *Burkholderiaceae*, *Betaproteobacteria*
 EI19 *Acinetobacter* sp. (DQ257432) 99%, *Moraxellaceae*, *Gammaproteobacteria*
 EI10 *Comamonas* sp. (AM937260) 99%, *Comamonadaceae*, *Betaproteobacteria*
 EI11 Uncultured bacterium clone EPR3967-02-Bc49 (EU491796) 90%, *Ralstoniaceae*, *Betaproteobacteria*
 EI12 *Chryseobacterium* sp. (DQ521273) 98%, *Flavobacteriaceae*, *Bacteroidetes*
 EI20 Uncultured *Comamonas* sp. clone MQ (HQ176411) 98%, *Comamonadaceae*, *Betaproteobacteria*
 EI22, 34, 44 Uncultured *Aquabacterium* sp. clone DS130 (DQ234213) 99%, Unclassified *Burkholderiales*, *Betaproteobacteria*
 EI23, 25, 31, 45 Uncultured bacterium isolate DGGE gel band B8 (HM068949) 97%, *Ralstoniaceae*, *Betaproteobacteria*
 EI21 *Pedobacter* sp. (DQ521273) 96%, *Sphingobacteriaceae*, *Bacteroidetes*
 EI32 Uncultured *Janthinobacterium* sp. clone 147 (GU202951) 99%, *Oxalobacteriaceae*, *Betaproteobacteria*
 EI33, 38 *Burkholderia* sp. (AB265148) 99%, *Burkholderiaceae*, *Betaproteobacteria*
 EI39 Uncultured *Oxalobacteraceae* bacterium clone BF64A_B63 (HM141157) 99%, *Oxalobacteriaceae*, *Betaproteobacteria*
 EI42 Uncultured beta proteobacterium clone A23YP01RM (FJ569567) 99%, *Ralstoniaceae*, *Betaproteobacteria*
 EI43 Uncultured bacterium clone nby240c04c1 (HM807869) 99%, *Comamonadaceae*, *Betaproteobacteria*
 EI46 *Comamonas* sp. (JF729307) 99%, *Comamonadaceae*, *Betaproteobacteria*
 EI47 *Pseudomonas* sp. (FN995245) 94%, *Pseudomonadaceae*, *Gammaproteobacteria*

Fig. S4 Denaturing gradient gel electrophoresis (DGGE) analysis of bacterial communities. (A) Bacterial communities from the Ligurian Sea (core KESC9-30) on a DGGE gradient of 25-55% denaturant. (B) Sequence similarities to the closest cultivated relatives. White numbered dots represent the bands that were excised and sequenced. M: marker.

BACTERIA

A RHS-KS-33



B Sequence similarity of excised DGGE bands

AR1 *Burkholderia* sp. (AF408997) 86%, *Burkholderiaceae*, *Betaproteobacteria*
 AR2 *Acinetobacter* sp. (AF408997) 93%, *Moraxellaceae*, *Gammaproteobacteria*
 AR8, 22, 64, BR37 Uncultured bacterium clone PT-AEXL-B25 (AB368999) 99%, *Propiniobacteriaceae*, *Actinobacteria*
 AR9 Uncultured bacterium clone FeC_1_E2 (FJ802354) 86%, *Burkholderiaceae*, *Betaproteobacteria*
 AR10 Uncultured bacterium clone3-111 (GU212458) 96%, *Burkholderiaceae*, *Betaproteobacteria*
 AR40, 99 Uncultured bacterium clone COREB 51 (EF562235) 93%, *Comamonadaceae*, *Betaproteobacteria*
 AR52 Uncultured bacterium clone P4s-145 (GQ329244) 99%, *Propiniobacteriaceae*, *Actinobacteria*
 AR78 Uncultured bacterium clone 26 (FJ534972) 93%, *Comamonadaceae*, *Betaproteobacteria*
 AR107, BR14 Uncultured bacterium clone ARN17 (AM936611) 98%, *Burkholderiaceae*, *Betaproteobacteria*
 BR8 Uncultured bacterium clone ncd773c10c1 (HM300328) 99%, *Propiniobacteriaceae*, *Actinobacteria*
 BR5, 31, 36, 45, 49, 67 Uncultured bacterium clone IS-191 (GQ339248) 99%, *Ralstoniaceae*, *Betaproteobacteria*
 BR17 Uncultured bacterium clone HN14 (FJ269052) 98%, unclassified *Burkholderiales*, *Betaproteobacteria*
 BR22 Uncultured bacterium clone PL26B10 (AY570561) 98%, *Bacteroidaceae*, *Bacteroidetes*
 BR32 Uncultured bacterium clone sliv-75 (FM877656) 98%, *Comamonadaceae*, *Betaproteobacteria*
 BR40 Uncultured *Bacteroidetes* bacterium 16S rRNA gene from clone QEEB1CD08 (CU917861) 98%, *Bacteroidaceae*, *Bacteroidetes*
 BR41, 76 *Bacteroides* sp. (AB547643) 98%, 99% *Bacteroidaceae*, *Bacteroidetes*
 BR47, 53 Uncultured bacterium clone 61-01-24c014 (DQ16809) 99%, Unclassified (*Bacteroidetes*)
 BR57 Uncultured bacterium clone *Staphylococcus* sp. (DQ837034) 96%, *Staphylococcaceae*, *Firmicutes*
 BR59 Uncultured beta proteobacterium clone Kir51grn dB7.2 (HM480181) 98%, *Comamonadaceae*, *Betaproteobacteria*
 BR63 *Ralstonia* sp. (HQ267096) 99%, *Ralstoniaceae*, *Betaproteobacteria*
 BR75 Uncultured bacterium clone ncd972a02c1 (HM331711) 99%, Unclassified (*Bacteroidetes*)
 BR77 Uncultured beta proteobacterium clone A23YP01RM (FJ569567) 99%, *Ralstoniaceae*, *Betaproteobacteria*

Fig. S5 Denaturing gradient gel electrophoresis (DGGE) analysis of bacterial communities. (A) Bacterial communities from the Gulf of Lions (RHS-KS-33) on a DGGE gradient of 30-60% denaturant. (B) Sequence similarities to the closest cultivated relatives. White numbered dots represent the bands that were excised and sequenced, and the grey dots represent the excised bands that migrated on a DGGE-GE gel (data not shown). M: marker.

ARCHAEA

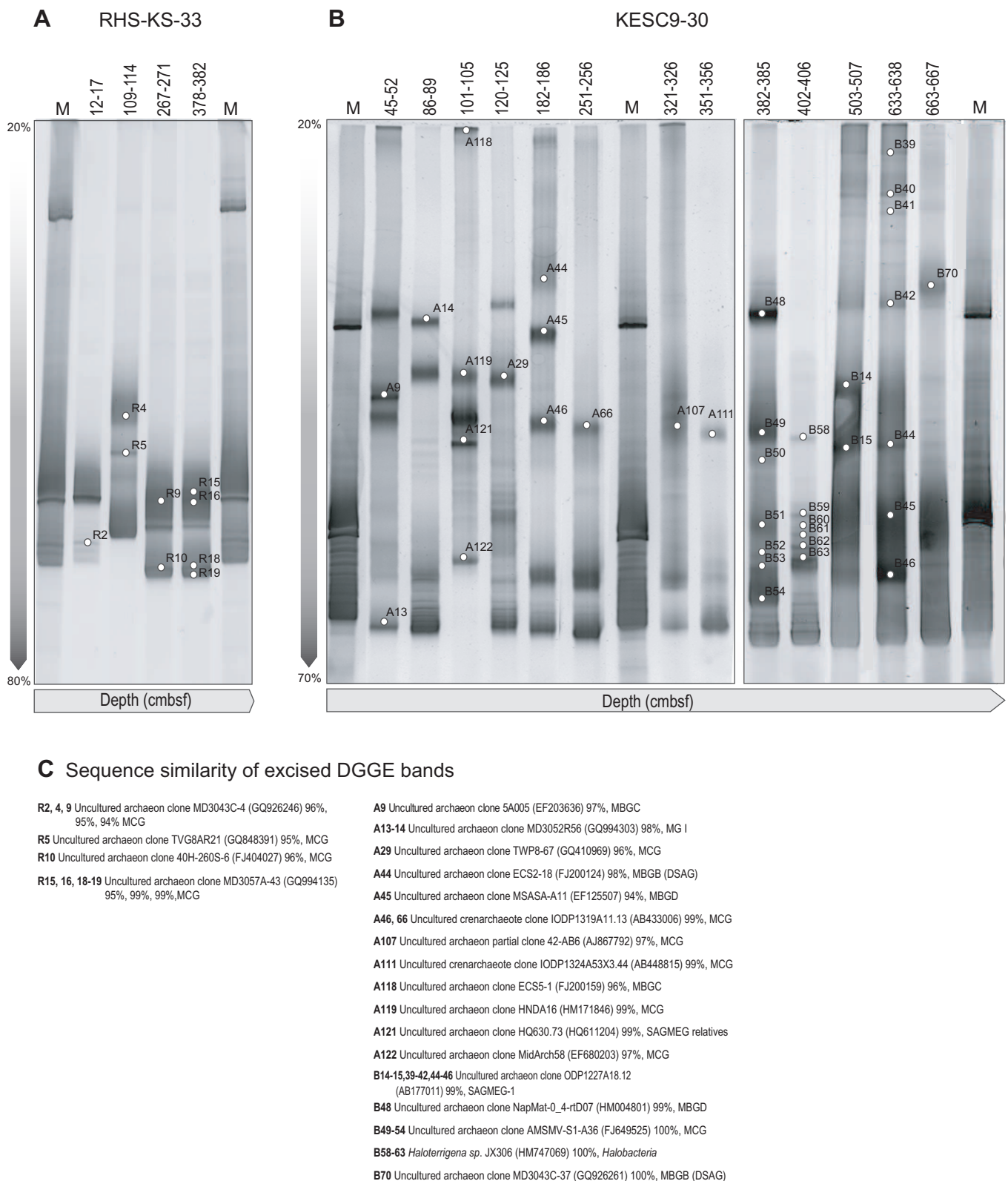
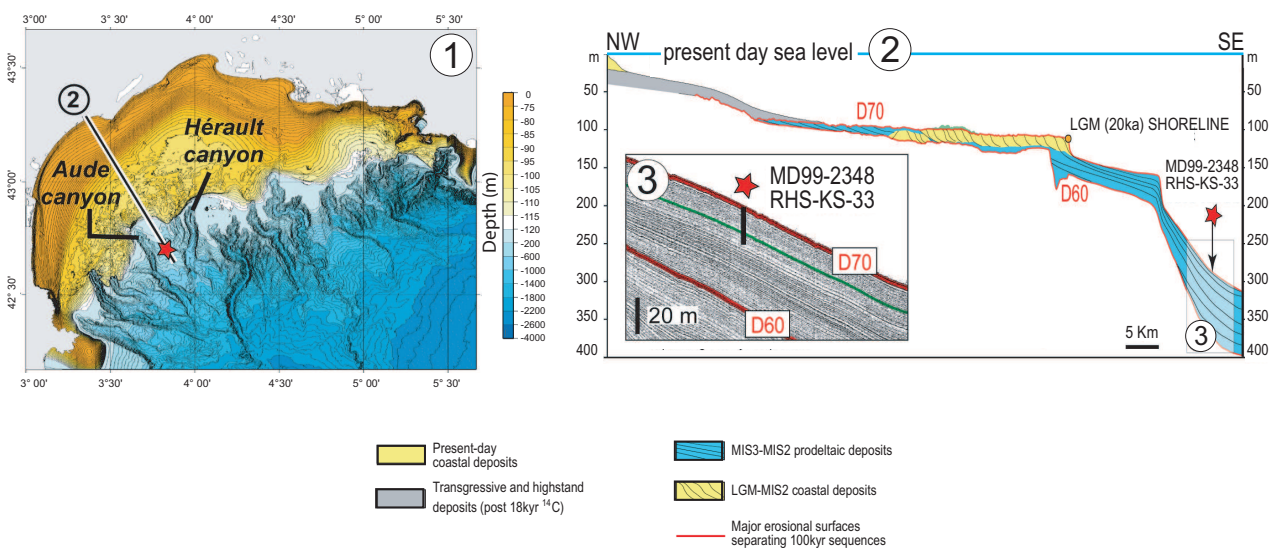


Fig. S6 Denaturing gradient gel electrophoresis (DGGE) analysis of archaeal communities. (A) Archaeal communities from the Gulf of Lions (RHS-KS-33) on a DGGE gradient of 20-80% denaturant, (B) Archaeal communities from the Ligurian Sea (core KESC9-30) on a DGGE gradient of 20-70% denaturant. (C) Sequence similarities to the closest cultivated relatives. White numbered dots represent the bands that were excised and sequenced. M: marker.

A Aude/Hérault interfluve area - Gulf of Lions



B Var Ridge - Ligurian Sea

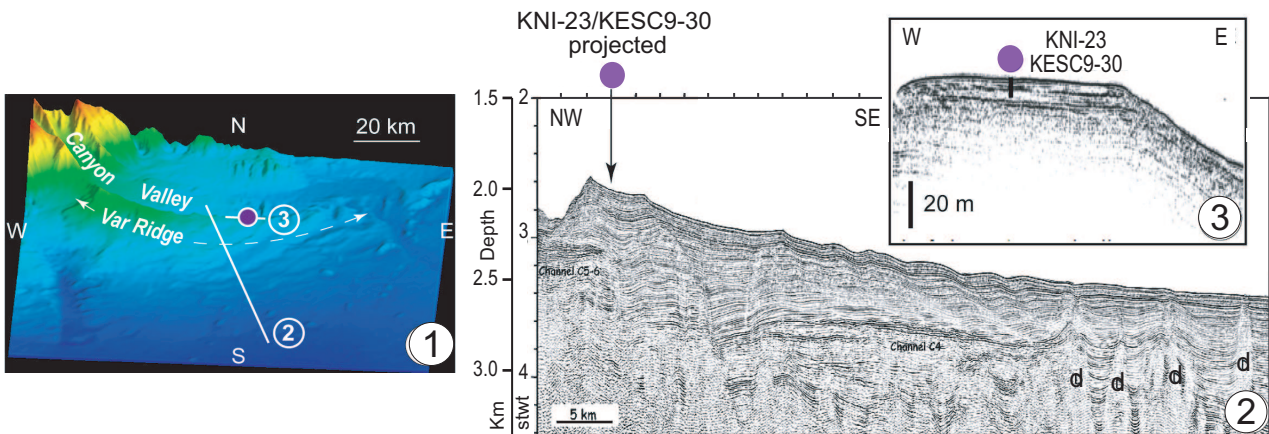


Fig.S7 A Gulf of Lions bathymetric map (1) and location of line drawing of Sparker profile shown in (2) (black line) on the upper slope between the Aude and Hérault canyons at the same location as twin core MD99-2348 (Beaudouin et al., 2005; Jouet et al., 2006; Sierro et al., 2009). (2) Line drawing of a Sparker seismic profile from the present day coast line to the outer shelf (modified from Rabineau et al., 2006, see location in (1)): RHS-KS-33 core sampled MIS2-early transgressive prodeltaic deposits. (3) Zoom of the Sparker seismic line in the area of RHS-KS-33, showing the non disturbed stratified seismic facies of the upper slope deposits. **B** The Var Ridge, in the Ligurian Sea. (1) 3D block diagram (modified from Jégou, 2004) showing the morphology of the Var Ridge and location of the Sparker seismic profiles (white lines) in (2) and (3) and the location of KESC9-30 core, same as twin core KNI-23 (Migeon et al., 2000; Jorry et al., 2011) (purple dot). (2) Sparker seismic profile (modified from Migeon et al., 2006) illustrating the architecture of the Var Ridge and the relative position of core KESC9-30 on top of the ridge; (d): salt domes at the southern part of the ridge. (3) Zoom of a sub-bottom profile (3.5 kHz) showing the irregularly stratified facies of turbidites of the ridge (modified from Jégou, 2004).